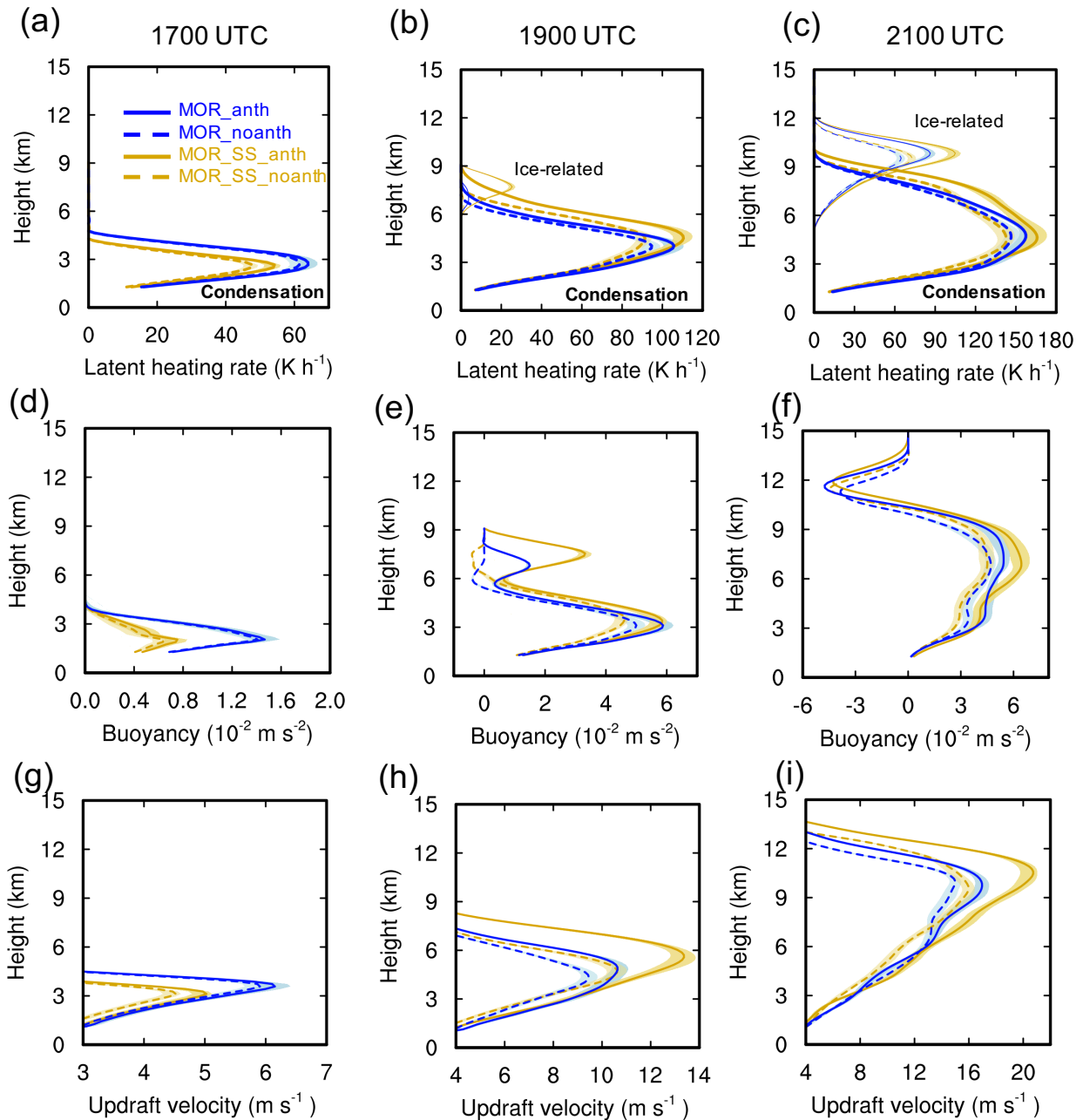Atmospheric
Chemistry
and Physics

Open Access

Supplement of

Impacts of cloud microphysics parameterizations on simulated aerosol–cloud interactions for deep convective clouds over Houston

Yuwei Zhang et al.

Correspondence to: Jiwen Fan (jiwen.fan@pnnl.gov)

Figure S1 Vertical profiles of (a-c) latent heating rate from condensation (weighted lines) and ice-related processes (freezing, riming, and deposition; thin lines), (d-f) buoyancy, (g-i) updraft velocity averaged over the top 25 percentiles (i.e., 75th to 100th) of the updrafts with value greater than 2 m s⁻¹ from the simulations MOR_anth, MOR_noanth, MOR_SS_anth, and MOR_SS_noanth over the analysis domain as shown in the red box in Figure 7 at 1700 UTC, 1900 UTC and 2100 UTC. Data are processed in the same way as Figure 11.
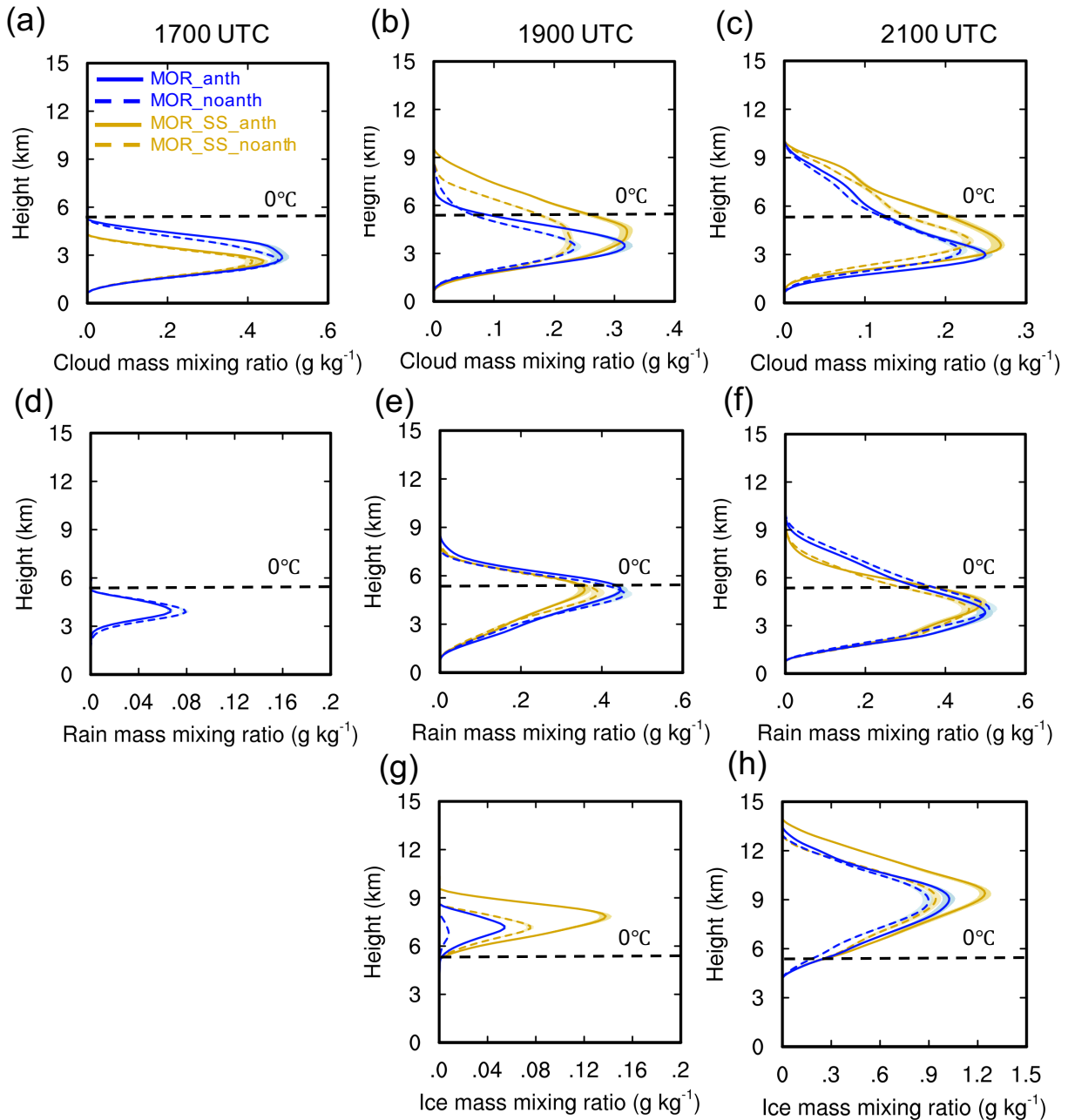
Figure S2 Vertical profiles mass mixing ratios of (a-c) cloud droplet, (d-f) rain drop and (g-h) ice particle (including ice, snow, and graupel) averaged over cloudy points (hydrometeor mass larger than 10^{-5} kg kg^{-1}) from the simulations MOR_anth, MOR_noanth, MOR_SS_anth, and MOR_SS_noanth over the analysis domain as shown in the red box in Figure 7 at 1700 UTC, 1900 UTC and 2100 UTC. Data are processed in the same way as Figure 11.
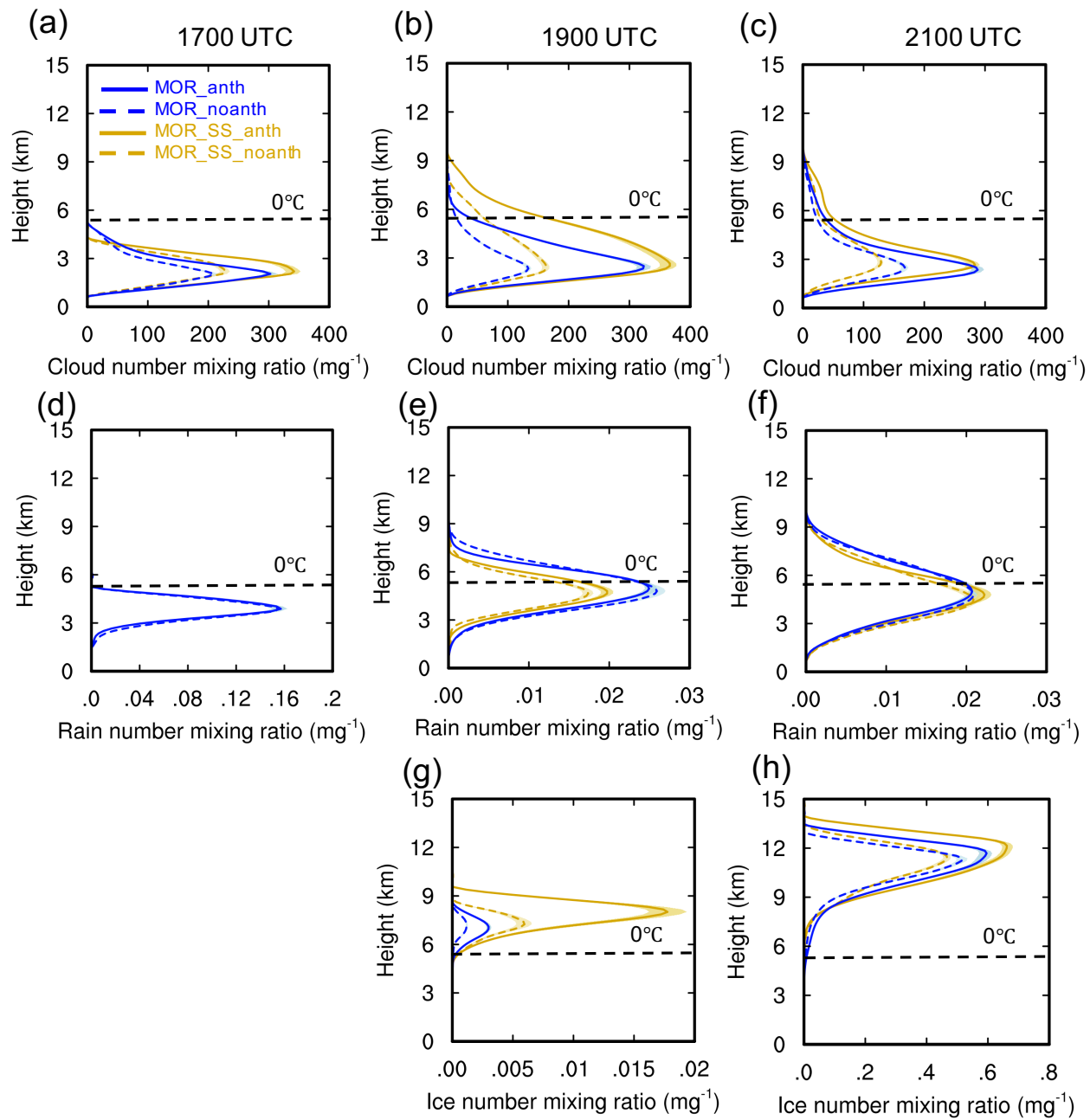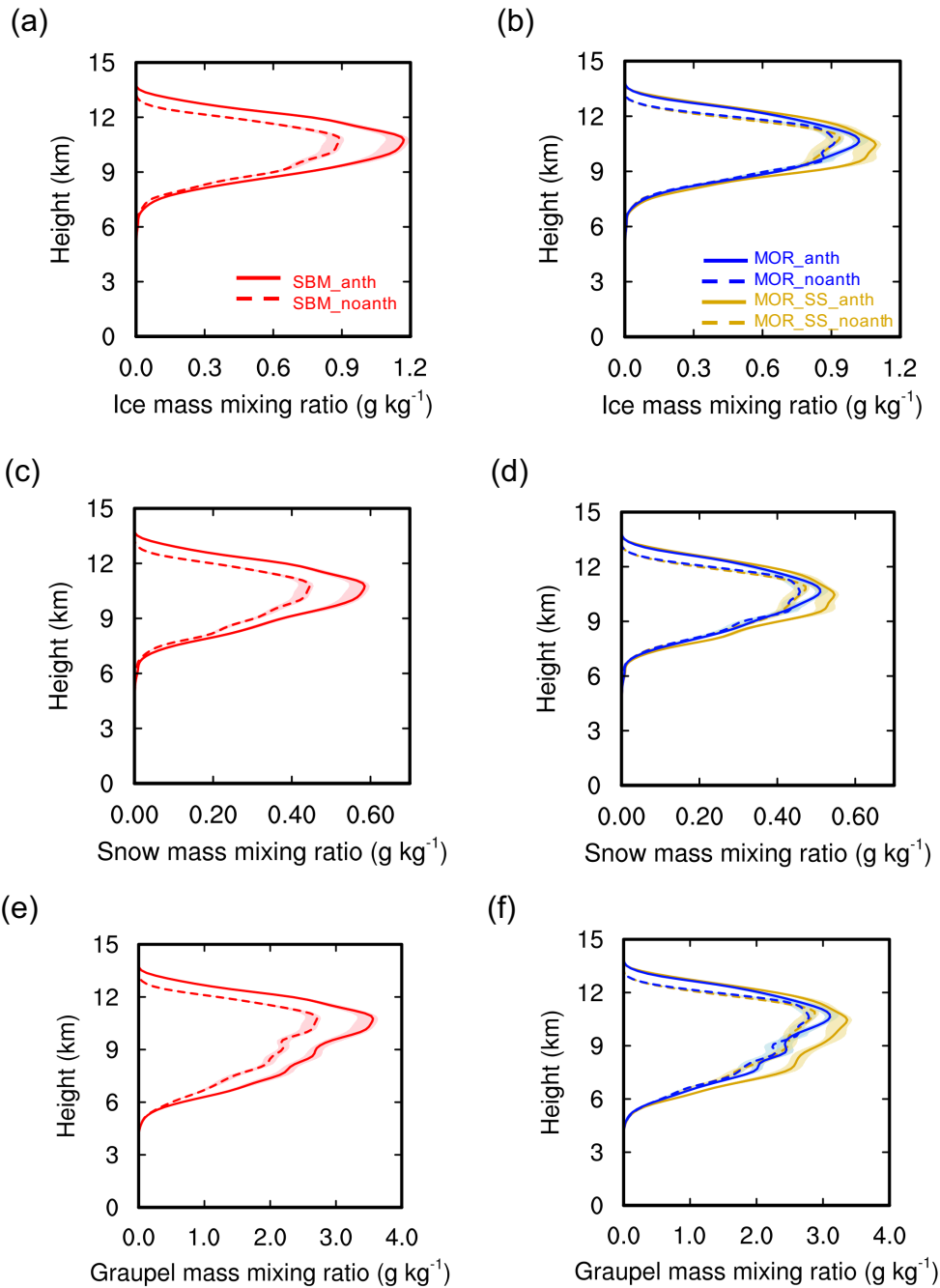
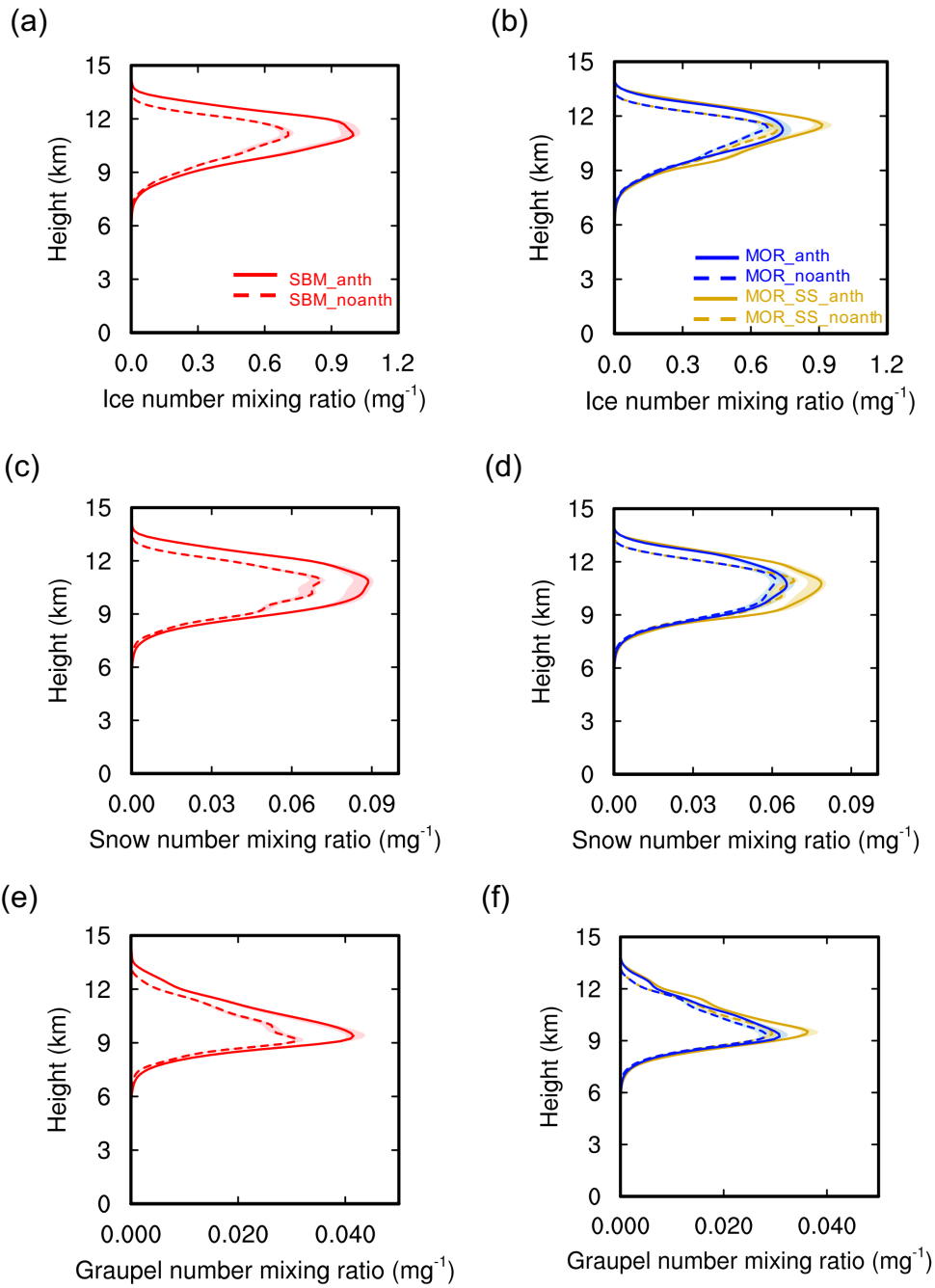**Figure S3** Same as Figure S2, but for hydrometeor number mixing ratio.

Figure S4 Vertical profiles of (a, b) ice, (c, d) snow and (e, f) graupel particle (mass mixing ratios averaged over the top 25 percentiles (i.e., 75th to 100th) of the updrafts with value greater than 2 m s^{-1} from the simulations SBM_anth and SBM_noanth (red), MOR_anth and MOR_noanth (blue), and MOR_SS_anth and MOR_SS_noanth (orange) over the study area (red box in Fig. 7) during the strong convection period (2000 – 2300 UTC, 19 Jun 2013). Data are processed in the same way as Figure 11.

(a)

(b)

(c)

(d)

(e)

(f)

Figure S5 Same as Figure S4, but for hydrometeor number mixing ratio.

45

46